Gold Dendrimer Encapsulated Nanoparticles as Labeling Agents for Multiwalled Carbon Nanotubes

M. Antonia Herrero,[†,‡] Javier Guerra,[†,§,∥] V. Sue Myers,[⊥] M. Victoria Gómez,[†,¶] Richard M. Crooks,[⊥,*] and Maurizio Prato[‡,*]

[†]Departamento de Química Orgánica, Facultad de Química, Universidad de Castilla-La Mancha, 13071 Ciudad Real, Spain, [‡]Center of Excellence for Nanostructured Materials, Department of Pharmaceutical Sciences, University of Trieste, Piazzale Europa 1, 34127 Trieste, Italy, [§]NanoDrugs, S.L., Paseo de la Innovación 1, Campus Universitario, 02071 Albacete, Spain, [∥]CIBERNED, Unidad Asociada Neurodeath, CSIC-Universidad de Castilla-La Mancha, Departamento de Ciencias Médicas, Facultad de Medicina, 02006 Albacete, Spain, [⊥]Department of Chemistry and Biochemistry, Center for Nano and Molecular Science and Technology, and the Texas Materials Institute, The University of Texas at Austin, 1 University Station, A5300, Austin, Texas 78712-0165, and [¶]Instituto Regional de Investigación Científica Aplicada (IRICA), Universidad de Castilla-La Mancha, 13071 Ciudad Real, Spain

ABSTRACT In this paper, we report the functionalization of the surface of multiwalled carbon nanotubes (MWNTs) with Au dendrimer encapsulated nanoparticles (DENs). The results show that, when pristine MWNTs having hydrophobic surfaces are exposed to DENs, the dendrimers aggregate on the MWNT surface. However, when the MWNTs are oxidized in acid prior to exposure to DENs, well-dispersed submonolayer coverages of Au nanoparticles are observed on the MWNT surface. This suggests that acid-induced debundling of the nanotubes is an essential prerequisite for attachment of nearly monodisperse DENs. Electron microscopy and NMR spectroscopy confirm that the structures of the DENs and dendrimers are retained after immobilization on the surface of acid-functionalized MWNTs.

KEYWORDS: dendrimer · gold nanoparticles · carbon nanotubes · nanomaterials

We report immobilization of Au dendrimer encapsulated nanoparticles (DENs)[1] onto the surface of multiwalled carbon nanotubes (MWNTs). Clear differences in terms of aggregation of Au were observed depending on the hydrophilic or hydrophobic character of the MWNTs. Attachment to an insoluble, hydrophobic MWNT resulted in aggregation of the Au particles. Therefore, immobilization of Au DENs onto the surface of the MWNTs requires that the latter be functionalized with carboxylic acid groups. This acidic functionalization leads to debundling of MWNTs and provides surface sites for interactions with amino groups present on the surface of the dendrimer. NMR spectroscopy and electron microscopy show that the structure of both dendrimers and the encapsulated nanoparticles, respectively, is preserved under our experimental conditions for the immobilization on the nanotube surface.

Poly(amidoamine) (PAMAM) dendrimers have been used to template monometallic,[1−7] alloy,[1,8,9] and core/shell[1,8] bimetallic, nanoparticles containing up to a few hundred atoms. The synthesis of DENs proceeds in two steps. First, metal ions are complexed to interior functional groups within the dendrimer. Second, chemical reduction of this precursor leads to particle formation. The nature of the chemical interactions between the $AuCl_4^-$ precursor and specific functional groups within the dendrimer has not been identified.[10,11] Nevertheless, it has been found that there is a direct correlation between the metal-ion-to-dendrimer ratio used in the synthesis and the size of gold DENs.[10,12−14] A variety of analytical methods, including electron microscopy,[10] NMR,[6,7] and selective catalysis experiments,[15−17] have been used to show that DENs reside within individual dendrimers. After reduction, the dendrimer serves as a protective agent to prevent aggregation of the nanoparticles which are hosted within the PAMAM cavities.[6,7,18,19]

Multiwalled carbon nanotubes are concentrically rolled graphene sheets composed of carbon hexagons having highly strained regions at the tips where pentagons are present. Because of their desirable properties, these nanomaterials have played a leading role in fields such as nanomedicine,[20−27] photophysics,[28−31] and sensing.[32,33] One of the main limitations of MWNTs is their poor solubility, which can be enhanced in polar solvents, such as dimethylformamide and water, by functionalizing their surfaces with polar groups.[34,35] However, excessive functionalization damages

*Address correspondence to crooks@cm.utexas.edu, prato@units.it.

Received for review November 30, 2009 and accepted January 18, 2010.

Published online January 29, 2010.
10.1021/nn901729d

the surface of CNTs and changes their physical properties. Dendrimers have previously been used as surface modifiers to improve the solubility of CNTs without damaging their carbon skeleton.[28,36−40] Specifically, it has been found that attachment of PAMAM dendrimer-like fragments increases the solubility of MWNTs in water[37,41] and of SWNTs in organic solvents, such as DMF or *o*-dichlorobenzene.[28] Likewise, the solubility of MWNTs[38−40] and SWNTs[38,39,42] is improved by immobilization of aryl-ether-type dendrimers, dendrimeric structures based on benzyl esters and amino polyesters.

Dendrimers have also been used to introduce new functionalities to CNTs. For example, there have been several examples in which dendrimers were used to immobilize metal and semiconductor nanoparticles on their surface.[42−48] Specifically, groups led by Imae and Zhu, respectively, attached PAMAM dendrimers as templates to introduce metal and metal oxide nanoparticles on the surface of MWNTs.[36,43,44] However, the metal nanoparticles were found to be too large to be fully encapsulated within individual dendrimers.[43,44] This suggested the presence of small aggregates of DENs or larger nanoparticles, surrounded by multiple dendrimers, which are known as dendrimer-stabilized nanoparticles (DSNs).[49] Likewise, Stevenson and Vijayaraghavan showed that preformed Pt nanoparticles stabilized by dendrimers can be immobilized on nitrogen-doped MWNTs.[45] Finally, Newkome and co-workers synthesized CdS quantum dots encapsulated within amino polyester dendrons and tethered them to SWNTs.[42]

The use of PAMAM dendrimer derivatives in nanomedicine[41,47,50−55] has been extensively studied. For example, divergent growth of PAMAM dendrons on CNT surfaces has been reported for several applications, including light harvesting with chromophores[28] and biomedical applications such as gene transfer[41] or antimicrobial therapy.[47] Presynthesized PAMAM dendrimers have also been immobilized on CNTs for applications to gene-transfer therapy.[21]

The key finding that emerges from this work is a procedure for attaching Au DENs to MWNTs that preserves the structure of both. Two important parameters are necessary to achieve these results. First, MWNTs must be at least partially soluble. For example, we have observed that the attachment of Au DENs onto pristine MWNTs (*p*-MWNTs), which are not soluble in water, leads to aggregation of the Au nanoparticles. Second, NMR spectroscopy shows that PAMAM dendrimers degrade when refluxed in water at 100 °C, and therefore elevated temperatures should be avoided during the immobilization process.

RESULTS AND DISCUSSION

Au DENs containing an average of ~200 atoms were encapsulated within sixth-generation, amine-terminated PAMAM dendrimers (G6-NH_2). These DENs, which we denote as G6-NH_2(Au_{200}), were synthesized according to a previously reported procedure.[56] TEM (transmission electron microscopy) analysis of these materials (Figure S1a,b in Supporting Information) indicates they have a size distribution of 2.0 ± 0.5 nm, which is consistent with previous results from our group and with the theoretical size calculated for cuboctahedral nanoparticles containing 200 Au atoms (1.9 nm).[13] UV−vis spectroscopic data (Figure S1c) indicate a monotonically decreasing absorbance toward higher wavelength and a very small plasmon band at 522 nm. These spectral properties are consistent with previous results and with Au DENs having diameters of ~2.0 nm.[10,12,13]

The MWNTs used in the present study have average outer and inner diameters of 20−30 and 5−10 nm, respectively. One important objective of this study was to examine the attachment of Au DENs to MWNTs as a function of the MWNT surface properties (Figure 1). The materials illustrated in Figure 1 were characterized by TEM, energy-dispersive X-ray spectroscopy (EDS), thermogravimetric analysis (TGA), X-ray photoelectron (XPS) spectroscopy, and the Kaiser test (for determination of free primary amino groups). It was not possible to obtain UV−vis spectra of the MWNT/DEN composites due to a strong background arising from light scattering (Figure S2).

Two different synthetic approaches have been used to prepare MWNT/DEN composites. In the first procedure, Au DENs were stirred with underivatized *p*-MWNTs in 10/1 H_2O/DMF at 40 °C for 24 h (top of Figure 1). In the second procedure, the MWNT surface was oxidized prior to exposure to the DENs by treating the *p*-MWNTs with a solution of H_2SO_4/HNO_3 (3/1) in the presence of ultrasound (25 min with a sonic tip, 750 W) followed by sonication for 5 h in a water bath. This procedure has been shown to yield MWNTs functionalized on their surfaces with carboxylic acid groups (*c*-MWNTs).[57−59] It also shortens the nanotubes and introduces edge sites. The composites were prepared by mixing *c*-MWNTs and Au DENs in 10/1 H_2O/DMF solutions at 40 °C for 24 h.

Figure 2a shows the dependence of the solubility on the chemical treatment of the MWNTs. The Au-*c*-MWNTs are rather soluble in water (~0.2 mg/mL), which is comparable to the findings of others.[58,60] The other materials have significantly lower solubilities: Au-*p*-MWNT, ~0.04 mg/mL, and *c*-MWNTs, ~0.06 mg/mL. In the case of Au-*p*-MWNT, the increase in their solubility is originated by the presence of amino-terminated PAMAM dendrimers on their structure. It has previously been shown that primary amino groups of organic molecules interact with the carbon surface of *p*-MWNTs,[61,62] giving rise to a slight improvement in their water solubility. The *p*-MWNTs are not soluble in water. The solubility of each material is related to its organizational structure in solution. Specifically, Figure S3a,b (Supporting Information) shows that *p*-MWNTs comprise en-

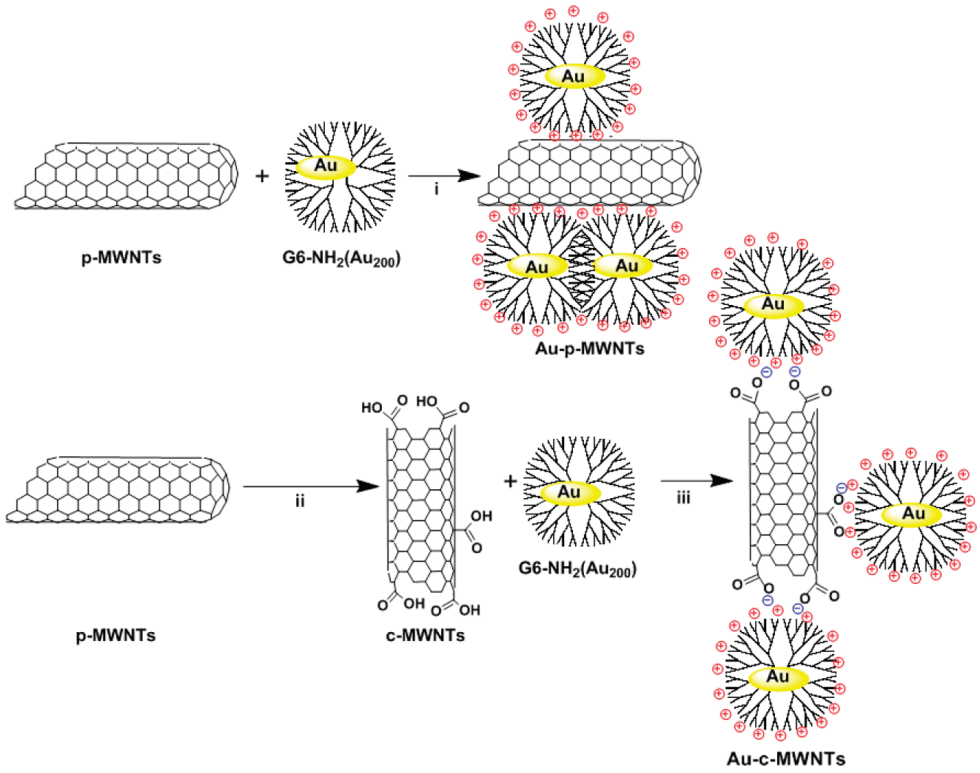

Figure 1. Reaction conditions: (i) water/DMF 10/1, 40 °C for 24 h; (ii) H_2SO_4/HNO_3 3/1, sonication for 25 min in a sonic tip followed by sonication in a water bath for 5 h; (iii) water/DMF 10/1, 40 °C for 24 h.

tangled tubes that form bundles. In contrast, *c*-MWNTs are debundled due to the presence of polar groups on their surface (Figure S3c).

Figure 2b shows that Au DENs aggregate on the surface of *p*-MWNTs. Particle size distributions (Figure S3d) of the resulting aggregates reveal a bimodal distribution of nanoparticles. The average size of ~30% of the Au particles is centered at 3.5 ± 0.3 nm, and the remaining ~70% is centered at 5.4 ± 1.1 nm. We do not fully understand why the Au DENs aggregate on the *p*-MWNTs surfaces, but their weak adsorption could be accompanied by high mobility. Similar findings, involving weak adsorption on nondefective carbon surfaces, have previously been reported by Vijayaraghavan and Stevenson and our own group.[45,63] Finally, ^{1}H NMR and pulsed-field gradient experiments, which are discussed later, indicate that the reaction conditions used for DEN im-

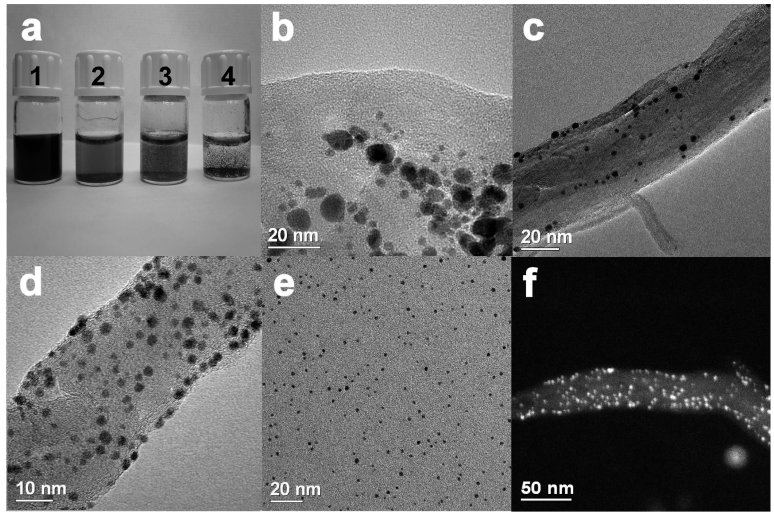

Figure 2. (a) Optical micrograph of vials containing aqueous solutions of MWNTs with and without DENs: 1, Au-*c*-MWNTs (0.2 mg/mL); 2, *c*-MWNTs (0.06 mg/mL); 3, Au-*p*-MWNTs (0.04 mg/mL); 4, *p*-MWNTs. TEM images of (b) Au-*p*-MWNTs; (c) and (d) Au-*c*-MWNTs. (e) TEM image of G6-$NH_2(Au_{200})$. (f) Representative high-angular annular dark-field STEM image of Au-*c*-MWNTs.

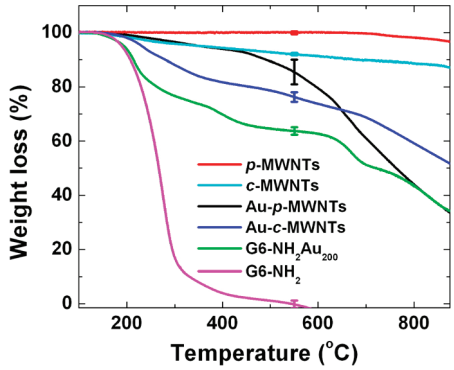

Figure 3. TGA of the dendrimers, Au DENs, and composites indicated in the legend. The measurements were performed under a N_2 atmosphere, and the heating rate was 10 °C/min.

mobilization need to be chosen with special care because they may lead to partial degradation of the dendrimers, and this could in turn lead to aggregation.[43,44,49]

In contrast to the *p*-MWNTs, Au DENs are well-dispersed on acid-treated MWNTs (Figure 2c,d). Acid pretreatment of the MWNTs generates surface carboxylic acid groups,[57,58] which enhances solubility and causes debundling of the individual nanotubes. We believe that a stronger adsorptive interaction between the positively charged dendrimers and the negatively charged MWNT surface leads to less surface mobility of the DENs and hence less aggregation. It is notable that the size of the Au DENs is the same before (2.0 ± 0.5 nm, Figure 2e and Supporting Information Figure S1a,b) and after (2.1 ± 0.5 nm, Figure S3f) electrostatic attachment to the acid-functionalized MWNT surface.

Figure 2f shows a STEM-HAADF (scanning transmission electron microscopy high-angular annular dark-field) image of the Au-*c*-MWNTs. The high nuclear density of the Au particles provides good contrast of the metal along the surface of the MWNT.[64] In future studies, this will facilitate the recognition of the MWNTs in the cellular media because cellular organelles have dimensions and electron contrast that are similar to MWNTs. Au DENs are suitable as biological markers as Baker and co-workers have recently shown.[65]

XPS experiments confirm the presence of Au in the DEN-containing composites (Figure S4). The presence of Fe and Ni was determined by means of EDX experiments (Figure S5). The latter two metals originate from the catalysts used to prepare the MWNTs.[24,59]

Figure 3 shows the thermogravimetric analysis (TGA) of the dendrimers, Au DENs, and the DEN/MWNT composites. Weight losses were measured at 550 °C because at this temperature metal-free PAMAM dendrimers are fully removed (purple line, Figure 3). These macromolecules are thermosensitive, and it has been reported that, in the presence of oxygen and metals, such as Pt, the decomposition is accelerated starting at temperatures as low as 75 °C.[66−68] However, we cannot exclude the possibility of organic residue on the MWNT surface, even at 550 °C.[68] Importantly, no decomposition of the *p*-MWNTs is observed until >700 °C (red line, Figure 3).[69] Therefore, the measured weight loss from each sample can be attributed to loss of dendrimer attached to the MWNT surface. The highest weight loss value (23.5 ± 0.9%), which corresponds to 4.0 ± 0.2 μmol G6-$NH_2(Au_{200})$/g *c*-MWNT, is obtained for Au-*c*-MWNTs. Au-*p*-MWNTs samples exhibited a weight loss of just 9.6 ± 4.5%, which corresponds to 1.6 ± 0.8 μmol G6-$NH_2(Au_{200})$/g *p*-MWNT. These results are in qualitative agreement with the TEM data, which revealed a higher surface concentration of Au DENs on Au-*c*-MWNTs.

Table 1 summarizes the results of the analytical techniques used to characterize the MWNTs and MWNT/DEN composites examined in this project. The results show that the uptake of Au DENs is substantially higher for *c*-MWNTs compared to the pristine nanotubes. For example, elemental analysis (EA) of Au-*c*-MWNT yields a total nitrogen content of 5.48 ± 0.15% g_N/g_{MWNT}. There are 1018 N atoms in each G6-NH_2 PAMAM dendrimer, thus the density of DENs is 3.8 ± 0.1 μmol G6-$NH_2(Au_{200})$/g *c*-MWNT. This value is in good agreement with the TGA results: 4.0 ± 0.2 μmol G6-$NH_2(Au_{200})$/g *c*-MWNT. We also performed on this sample the Kaiser test to prove the presence of free primary amino groups on the MWNT surface. This test is a qualitative analysis and is based on the reaction of ninhydrin with primary amines, which produces a characteristic dark blue compound.[70,71] As expected, the test was positive in the materials containing PAMAM dendrimers, Au-*p*-MWNTs and Au-*c*-MWNTs. In contrast, *p*-MWNTs and *c*-MWNTs gave no color when exposed to ninhydrin.

The mild conditions (40 °C, 24 h) used for immobilization of the DENs yielded a lower degree of functionalization (~4 μmol G6-$NH_2(Au_{200})$/g *c*-MWNT) relative to

TABLE 1. TGA, Elemental Analysis of the MWNTs, and DEN/MWNT Composites Reported in This Work

sample	TGA (% weight loss)	EA[a] (μmol Au DEN/g MWNT)	solubility (mg/mL)	Au DEN size (nm)
p-MWNTs	0.1 ± 0.07		ns[b]	
c-MWNTs	8.3 ± 0.6		0.06	
Au-*p*-MWNTs	9.6 ± 4.5	1.2 ± 0.2	0.04	3.5 ± 0.3[d]
	(1.6 ± 0.8)[c]			5.4 ± 1.1[e]
Au-*c*-MWNTs	23.5 ± 0.9 (4.0 ± 0.2)[d]	3.8 ± 0.1	0.20	2.1 ± 0.5

[a]Elemental analysis. [b]Not soluble. [c]Weight loss measured in μmol Au DEN/g MWNT. [d]70%. [e]30% of the sample population.

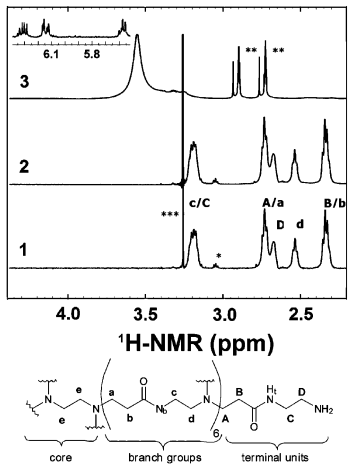

Figure 4. (Top) ^{1}H NMR spectra of G6-NH_2 recorded at 25 °C in D_2O (spectrum 1), at 40 °C for 24 h in D_2O (spectrum 2), and at reflux of DMF-d_7 for 48 h (spectrum 3). The intensity of the inset in spectrum 3 has been increased (2.5 times) for better visualization. (Bottom) Schematic representation of G6-NH_2 indicating the lettering scheme used to identify the methylene and nitrogen groups in the dendrimer. The peak marked with a single asterisk arises from impurities in the dendrimer solution. Peaks marked with a double asterisk correspond to the residual protons of the DMF-d_7 solvent. The peak marked with a triple asterisk comes from residual methanol present in the commercial dendrimer solution. Increasing the intensities of spectra 1 and 2 for a better visualization of all peaks results in an overlapping of the methanol peak with spectra 2 and 3.

other synthetic methods.[43,44] However, to preserve the integrity of the dendrimers, the conditions used in our experiments were mild compared to others reported in the literature (*e.g.*, DMF reflux, 2 days).[43,44] Our low degree of functionalization is comparable with results previously reported for attachment of dendrimer-templated platinum particles also performed under mild conditions.[45] Specifically, it is known that PAMAM dendrimers are thermolabile, and that the retro-Michael reaction is favored at high temperatures.[72−76]

Figure 4 shows NMR spectra of G6-NH_2 solutions in water and DMF at different temperatures. Spectrum 1 is a ^{1}H NMR spectrum obtained from an aqueous solution of G6-NH_2. The peak assignments were made using information obtained from complementary experiments, including ^{1}H−^{1}H COSY, ^{1}H−^{13}C HSQC, and ^{1}H−^{13}C HMBC.[77] Spectrum 2 is identical to spectrum 1, except that it was obtained after heating the aqueous G6-NH_2 solution to 40 °C for 24 h. Comparison of spectra 1 and 2 using sodium acetate as an internal standard indicates that ~85% of the dendrimer remains unaltered by the heating. The increase in the signal of minor alkyl fragments at 3.05 ppm confirms some decomposition of the dendrimeric structure. As mentioned previously, this level of decomposition might be sufficient to lead to some nanoparticle aggregation on the *p*-MWNT surfaces. Spectrum 3 is the ^{1}H NMR spectrum of a G6-NH_2 solution after being heated at dimethylformamide-d_7 reflux for 48 h.[43,44] After exposure to these conditions, there is significant degradation of the dendrimer, which is signaled by the appearance of new olefin fragment peaks at 5−7 ppm and new alkyl group peaks at 3.1−3.5 ppm. When G6-NH_2 is heated to reflux in D_2O, similar results were extracted from the ^{1}H NMR experiment (Supporting Information Figure S6). New peaks assigned to olefins at 5−7 ppm and signals at lower chemical shifts (~2.6 ppm) were also detected. This is a consequence of some dendrimer degradation resulting from the heating process. These results confirm that low temperatures and short reaction times with MWNTs are necessary to preserve the structure of the PAMAM dendrimers, and therefore the encapsulated Au nanoparticles, during the immobilization process.

Pulsed-field gradient spin−echo (PFGSE) NMR experiments were also carried out to determine if particular reaction conditions induced dendrimer degradation. PFGSE NMR is a valuable tool for mixture analysis because it distinguishes different species depending on their diffusion coefficients and therefore on their hydrodynamic radii.[78] Figures S7−S9 in Supporting Information show the pseudo-2D DOSY plots for 100 μM D_2O solutions of G6-NH_2 at 25 °C (Figure S7), after being heated to 40 °C for 24 h (Figure S8), and after being heated at D_2O reflux for 24 h (Figure S9). Figure S8 shows that mainly all of the dendrimer molecules remain unaltered since only a couple of signals around 3.0 ppm appear with a similar diffusion coefficients to the dendrimer. However, in Figure S9, different new signals with higher diffusion coefficient than the dendrimer itself are observed around 2.6 ppm, confirming the degradation of the dendrimer at high temperature and the importance of choosing the right experimental conditions for the electrostatic attachment of Au DENs.

CONCLUSIONS

Mild reaction conditions during Au DEN attachment and high MWNT solubility are key factors for obtaining monodisperse Au nanoparticles fully distributed along the MWNT surface. We showed that an increase in the temperature during the dendrimer attachment results in decomposition of the PAMAM structure, very likely because of the occurrence of a retro-Michael reaction. The insolubility of nonfunctionalized carbon nanomaterials leads to a high local concentration of Au DENs on the entangled MWNT bundles, resulting in the presence of Au aggregates on the nanotube surface. The particle coverages obtained for MWNT/DEN composites at the lower temperatures used here are sufficient for the biomedical applications we envision. Specifically, experiments are presently being carried out in our laboratories to study the behavior of the MWNTs as carriers for drug delivery, gene transfer, and image contrast agents.

MATERIALS AND METHODS

Chemicals. G6-NH_2 was purchased as a 5 wt % methanol solution (Dendritech, Inc., Midland, MI). The methanol was removed under vacuum prior to use, and 18 MΩ · cm Milli-Q deionized water (Millipore) was added to obtain aqueous solutions of G6-NH_2 having the desired concentrations. MWNTs were purchased from Nanostructured & Amorphous Materials Inc., Houston, TX; Stock No. 1240XH, 95%, OD 20−30 nm). $HAuCl_4$, $NaBH_4$ (99.9%, Reagent Plus), anhydrous dimethylformamide, D_2O (99.98%), and deuterated dimethylformamide (DMF-d_7) (Sigma-Aldrich, Inc.) were used as received. All experiments were carried out in air unless specified otherwise.

Characterization. TEM experiments were performed using a FEI Tecnai G2 F20 transmission electron microscope, equipped with Schottky-type field emission gun, X-twin lenses, an EDAX energy-dispersive X-ray spectrometer (EDS), and a scanning TEM (STEM) unit with high-angle annular dark-field (HAADF) detector operating at 200 kV. Samples were prepared by sonication for 10 min and dropwise (8 μL) addition of the sample onto a carbon-coated 400 mesh Cu grid (EM Sciences, Gibbstown, NJ) followed by solvent evaporation in air.

Thermogravimetric analyses were obtained using a TGA Q50 (TA Instruments) and recorded under N_2 by equilibrating at 100 °C followed by a ramp of 10 °C/min up to 1000 °C.

Elemental analyses were performed on a LECO CHNS-932 instrument.

XPS data were collected on a Kratos Axis Ultra DLD spectrometer using an Al Kα X-ray source. The spectra were collected with a pass energy of 160 eV and a resolution of 1 eV for survey spectra and with a pass energy of 20 eV and a resolution 0.1 eV for high-resolution spectra. Dwell times were 1.00 s in all instances. Samples were prepared by dropping the sample solutions onto Si wafers and allowing to dry.

NMR experiments were carried out using a Varian, Unity Inova NMR spectrometer operating at 499.7722 MHz for ^1H and at 152.678 MHz for ^{13}C. The spectrometer was equipped with a gradient amplifier and a four-nucleus 5 mm $^1H\{^{15}N-^{31}P\}$PFG high-field indirect detection probe. A presaturation pulse sequence was used to minimize the water peak in the 1D experiment. All 1D ^1H experiments (presaturation) and 2D experiments (COSY, HMBC, HSQC) were performed at 298 K using standard pulse sequences from the Varian library. Deuterated water (D_2O, 99.98%, Sigma-Aldrich, Inc.) and deuterated dimethylformamide (DMF-d_7, Sigma-Aldrich, Inc.) were used as solvent to perform the corresponding experiments of dendrimer stability. Sodium acetate (1.5 mM) was used as an internal standard and was added after cooling the solutions to 298 K.

Diffusion (PFGSE) experiments were performed at 298 K using the bipolar stimulated echo sequence with 32 increments in the gradient strength (2−95%), typically 64 averages per increment step, and 100 ms diffusion times. Pseudo-2D DOSY plots were processed with the standard Varian Software VNMR6.1C.

Peak assignments for G6-NH_2 were made using solutions containing 100 μM dendrimer: ^1H NMR (499.772 MHz, D_2O) δ (ppm) 3.19 (br t, 504H, H_c), 3.15 (br t, 512H, H_C), 2.71 (t, 1016H, $^3J_{H,H}$ = 5.0 Hz, $H_{A/a}$), 2.64 (br t, 512H, H_D), 2.52 (t, 504H, $^3J_{H,H}$ = 5.0 Hz, H_d), 2.32 (br t, 1016H, $H_{B/b}$).

Synthesis of Au DENs. Twenty milliliters of 2.0 μM G6-NH_2(Au_{200}) DENs were prepared according to a previous report.[56] Briefly, 0.8 mL of a freshly prepared, aqueous 10.0 mM $HAuCl_4$ solution was added to a 2.0 μM (final concentration) aqueous G6-NH_2 solution (18.76 mL). The metal−dendrimer complex solution was stirred for less than 1 min before a 5-fold molar excess (0.04 mL) of freshly prepared, aqueous 1 M $NaBH_4$ dissolved in 0.3 M NaOH was added. The vial was then sealed. Reduction occurs almost immediately and is accompanied by a change in color from pale yellow to wine red.

Synthesis of Au-*p*-MWNTs. Twenty milligrams of *p*-MWNTs were suspended in 5 mL of DMF and sonicated in a sonic bath for 10 min. Dropwise addition of the 2.0 μM Au DENs solution in water (2 × 25 mL, pH 7.5) was then performed. The reaction mixture was heated at 40 °C for 1 day. Subsequently, it was filtered using a Millipore system (GTTP 0.2 μm filter) and washed with methanol and water.

Synthesis of *c*-MWNTs. Five hundred milligrams of pristine MWNTs were sonicated (using a sonic tip) for 25 min in 125 mL of a 3/1 v/v mixture of concentrated H_2SO_4 and HNO_3, and then in a water bath for 5 h. The resulting suspension was diluted with water, filtered using Millipore system (GTTP 0.2 μm filter), washed with water until the pH was ~6, and then rinsed with methanol and dried under vacuum at 298 K.

Synthesis of Au-*c*-MWNTs. Twenty milligrams of *c*-MWNTs were dispersed in 5 mL of DMF followed by dropwise addition of a 2.0 μM aqueous solution of G6-NH_2(Au_{200}) (2 × 25 mL, pH 7.5). The reaction mixture was heated at 40 °C for 1 day. Subsequently, it was filtered using a Millipore system (GTTP 0.2 μm filter) and washed with methanol and water.

Acknowledgment. M.P. acknowledges the University of Trieste, INSTM, and MUR (PRIN 2006, prot. 2006034372 and Firb RBIN04HC3S). R.M.C. and V.S.M. thank the U.S. National Science Foundation (Grant 0847957) and the Robert A. Welch Foundation (Grant F-0032) for support of this project. M.A.H. and J.G. are indebted to the Junta de Comunidades de Castilla-La Mancha (Spain) for a postdoctoral research grant. J.G. acknowledges Prof. V. Ceña for funding (NanoDrugs, S.L.). M.V.G. also acknowledges MICINN and Marie Curie Reintegration Grants for financial support. Authors acknowledge Dr. A.H. Velders (University of Twente) for useful discussion related to NMR data. We also thank Dr. Domingo Ferrer of the Texas Materials Institute at UT-Austin and Claudio Gamboz of Settore Microscopia Elettronica at University of Trieste for their help with the TEM measurements.

Supporting Information Available: TEM micrographs, size distribution histograms, and UV−vis spectra of G6-NH_2(Au_{200}); UV−vis spectra of *p*-MWNTs, *c*-MWNTs, Au-*p*-MWNTs, and Au-*c*-MWNTs; TEM micrographs, EDX spectra, and size distribution histograms, and XPS spectra for MWNTs and MWNT/DEN composites; ^1H NMR spectra and pseudo-2D DOSY plots for G6-NH_2 after exposure to D_2O at different temperatures. This material is available free of charge *via* the Internet at http://pubs.acs.org.

REFERENCES AND NOTES

1. Scott, R. W. J.; Wilson, O. M.; Crooks, R. M. Synthesis, Characterization and Applications of Dendrimer-Encapsulated Nanoparticles. *J. Phys. Chem. B* **2005**, *109*, 692–704.
2. Knecht, M. R.; Crooks, R. M. Magnetic Properties of Dendrimer-Encapsulated Iron Nanoparticles Containing an Average of 55 and 147 Atoms. *New J. Chem.* **2007**, *31*, 1349–1353.
3. Knecht, M. R.; Garcia-Martinez, J. C.; Crooks, R. M. Synthesis, Characterization, and Magnetic Properties of Dendrimer-Encapsulated Nickel Nanoparticles Containing <150 Atoms. *Chem. Mater.* **2006**, *18*, 5039–5044.
4. Knecht, M. R.; Weir, M. G.; Myers, V. S.; Pyrz, W. D.; Ye, H.; Petkov, V.; Buttrey, D. J.; Frenkel, A. I.; Crooks, R. M. Synthesis and Characterization of Pt Dendrimer-Encapsulated Nanoparticles: Effect of the Template on Nanoparticle Formation. *Chem. Mater.* **2008**, *20*, 5218–5228.
5. Petkov, V.; Bedford, N.; Knecht, M. R.; Weir, M. G.; Crooks, R. M.; Tang, W.; Henkelman, G.; Frenkel, A. Periodicity and Atomic Ordering in Nanosized Particles of Crystals. *J. Phys. Chem. C* **2008**, *112*, 8907–8911.
6. Gomez, M. V.; Guerra, J.; Velders, A. H.; Crooks, R. M. NMR Characterization of Fourth-Generation PAMAM Dendrimers in the Presence and Absence of Palladium Dendrimer-Encapsulated Nanoparticles. *J. Am. Chem. Soc.* **2009**, *131*, 341–350.
7. Gomez, M. V.; Guerra, J.; Myers, V. S.; Crooks, R. M.; Velders, A. H. Nanoparticle Size Determination by ^1H NMR Spectroscopy. *J. Am. Chem. Soc.* **2009**, *131*, 14634–14635.
8. Knecht, M. R.; Weir, M. G.; Frenkel, A. I.; Crooks, R. M. Structural Rearrangement of Bimetallic Alloy PdAu Nanoparticles within Dendrimer Templates To Yield Core/Shell Configurations. *Chem. Mater.* **2008**, *20*, 1019–1028.

9. Ye, H.; Crooks, R. M. Effect of Elemental Composition of PtPd Bimetallic Nanoparticles Containing an Average of 180 Atoms on the Kinetics of the Electrochemical Oxygen Reduction Reaction. *J. Am. Chem. Soc.* **2007**, *129*, 3627–3633.
10. Gröhn, F.; Bauer, B. J.; Akpalu, Y. A.; Jackson, C. L.; Amis, E. J. Dendrimer Templates for the Formation of Gold Nanoclusters. *Macromolecules* **2000**, *33*, 6042–6050.
11. Knecht, M. R.; Garcia-Martinez, J. C.; Crooks, R. M. Hydrophobic Dendrimers as Templates for Au Nanoparticles. *Langmuir* **2005**, *21*, 11981–11986.
12. Torigoe, K.; Suzuki, A.; Esumi, K. Au(III)−PAMAM Interaction and Formation of Au−PAMAM Nanocomposites in Ethyl Acetate. *J. Colloid Interface Sci.* **2001**, *241*, 346–356.
13. Kim, Y. G.; Garcia-Martinez, J. C.; Crooks, R. M. Electrochemical Properties of Monolayer-Protected Au and Pd Nanoparticles Extracted from within Dendrimer Templates. *Langmuir* **2005**, *21*, 5485–5491.
14. Garcia-Martinez, J. C.; Crooks, R. M. Extraction of Au Nanoparticles Having Narrow Size Distributions from within Dendrimer Templates. *J. Am. Chem. Soc.* **2004**, *126*, 16170–16178.
15. Niu, Y.; Yeung, L. K.; Crooks, R. M. Size-Selective Hydrogenation of Olefins by Dendrimer-Encapsulated Palladium Nanoparticles. *J. Am. Chem. Soc.* **2001**, *123*, 6840–6846.
16. Niu, Y.; Crooks, R. M. Dendrimer-Encapsulated Metal Nanoparticles and Their Applications to Catalysis. *C. R. Chimie* **2003**, *6*, 1049–1059.
17. Oh, S.-K.; Niu, Y.; Crooks, R. M. Size-Selective Catalytic Activity of Pd Nanoparticles Encapsulated within End-Group Functionalized Dendrimers. *Langmuir* **2005**, *21*, 10209–10213.
18. Petkov, V.; Parvanova, V.; Tomalia, D.; Swansonb, D.; Bergstromb, D.; Vogt, T. 3D Structure of Dendritic and Hyper-Branched Macromolecules by X-ray Diffraction. *Solid State Commun.* **2005**, *134*, 671–675.
19. Liu, Y.; Bryantsev, V. S.; Diallo, M. S.; Goddard, W. A., III. PAMAM Dendrimers Undergo pH Responsive Conformational Changes without Swelling. *J. Am. Chem. Soc.* **2009**, *131*, 2798–2799.
20. Lacerda, L.; Ali-Boucetta, H.; Herrero, M. A.; Pastorin, G.; Bianco, A.; Prato, M.; Kostarelos, K. Tissue Histology and Physiology Following Intravenous Administration of Different Types of Functionalized Multiwalled Carbon Nanotubes. *Nanomedicine* **2008**, *3*, 149–161.
21. Pan, B. f.; Cui, D. x.; Xu, P.; Chen, H.; Liu, F. t.; Li, Q.; Huang, T.; You, X. g.; Shao, J.; Bao, C. c.; Gao, F.; He, R.; Shu, M. j.; Ma, Y. j. Design of Dendrimer Modified Carbon Nanotubes for Gene Delivery. *Chin. J. Cancer Res.* **2007**, *19*, 1–6.
22. Pantarotto, D.; Singh, R.; McCarthy, D.; Erhardt, M.; Briand, J. P.; Prato, M.; Kostarelos, K.; Bianco, A. Functionalized Carbon Nanotubes for Plasmid DNA Gene Delivery. *Angew. Chem., Int. Ed.* **2004**, *43*, 5242–5246.
23. Pantarotto, D.; Partidos, C. D.; Hoebeke, J.; Brown, F.; Kramer, E.; Briand, J. P.; Muller, S.; Prato, M.; Bianco, A. Immunization with Peptide-Functionalized Carbon Nanotubes Enhances Virus-Specific Neutralizing Antibody Responses. *Chem. Biol.* **2003**, *10*, 961–966.
24. Lacerda, L.; Soundararajan, A.; Singh, R.; Pastorin, G.; Al-Jamal, K. T.; Turton, J.; Frederik, P.; Herrero, M. A.; Li, S.; Bao, A.; Emfietzoglou, D.; Mather, S.; Phillips, W. T.; Prato, M.; Bianco, A.; Goins, B.; Kostarelos, K. Dynamic Imaging of Functionalized Multi-Walled Carbon Nanotube Systemic Circulation and Urinary Excretion. *Adv. Mater.* **2008**, *20*, 225–230.
25. Peer, D.; Krap, J. M.; Hong, S.; Farokhzad, O. C.; Margalit, R.; Langer, R. Nanocarriers as an Emerging Platform for Cancer Therapy. *Nat. Nanotechnol.* **2007**, *2*, 751–760.
26. Bianco, A.; Kostarelos, K.; Prato, M. Opportunities and Challenges of Carbon-Based Nanomaterials for Cancer Therapy. *Expert Opin. Drug Delivery* **2008**, *5*, 331–342.
27. Tasis, D.; Tagmatarchis, N.; Bianco, A.; Prato, M. Chemistry on Carbon Nanotubes. *Chem. Rev.* **2006**, *106*, 1105–1136.
28. Campidelli, S.; Sooambar, C.; Lozano Diz, E.; Ehli, C.; Guldi, D. M.; Prato, M. Dendrimer-Functionalized Single-Wall Carbon Nanotubes: Synthesis, Characterization, and Photoinduced Electron Transfer. *J. Am. Chem. Soc.* **2006**, *128*, 12544–12552.
29. Alvaro, M.; Atienzar, P.; de la Cruz, P.; Delgado, J. L.; Troiani, V.; Garcia, H.; Langa, F.; Palkar, A.; Echegoyen, L. Synthesis, Photochemistry, and Electrochemistry of Single-Wall Carbon Nanotubes with Pendent Pyridyl Groups and of Their Metal Complexes with Zinc Porphyrin. Comparison with Pyridyl-Bearing Fullerenes. *J. Am. Chem. Soc.* **2006**, *128*, 6626–6635.
30. Alvaro, M.; Atienzar, P.; de la Cruz, P.; Delgado, J. L.; Garcia, H.; Langa, F. Sidewall Functionalization of Single-Walled Carbon Nanotubes with Nitrile Imines. Electron Transfer from the Substituent to the Carbon Nanotube. *J. Phys. Chem. B* **2004**, *108*, 12691–12697.
31. Guldi, D. M.; Rahman, G. M. A.; Zerbetto, F.; Prato, M. Carbon Nanotubes in Electron Donor−Acceptor Nanocomposites. *Acc. Chem. Res.* **2005**, *38*, 871–878.
32. Katz, E.; Willner, I. Biomolecule-Functionalized Carbon Nanotubes: Applications in Nanobioelectronics. *ChemPhysChem* **2004**, *5*, 1084–1104.
33. Stampfer, C.; Helbling, T.; Obergfell, D.; Schoberle, B.; Tripp, M. K.; Jungen, A.; Roth, S.; Bright, V. M.; Hierold, C. Fabrication of Single-Walled Carbon-Nanotube-Based Pressure Sensors. *Nano Lett.* **2006**, *6*, 233–237.
34. Georgakilas, V.; Kordatos, K.; Prato, M.; Guldi, D. M.; Holzinger, M.; Hirsch, A. Organic Functionalization of Carbon Nanotubes. *J. Am. Chem. Soc.* **2002**, *124*, 760–761.
35. Kordatos, K.; Da Ros, T.; Bosi, S.; Vázquez, E.; Bergamin, M.; Cusan, C.; Pellarini, F.; Tomberli, V.; Baiti, B.; Pantarotto, D.; Georgakilas, V.; Spalluto, G.; Prato, M. Novel Versatile Fullerene Synthons. *J. Org. Chem.* **2001**, *66*, 4915–4920.
36. Shen, Y.; Xu, Q.; Gao, H.; Zhu, N. Dendrimer-Encapsulated Pd Nanoparticles Anchored on Carbon Nanotubes for Electro-Catalytic Hydrazine Oxidation. *Electrochem. Commun.* **2009**, *11*, 1329–1332.
37. Cao, L.; Yang, W.; Yang, J. W.; Wang, C. C.; Fu, S. K. Hyperbranched Poly(amidoamine)-Modified Multi-Walled Carbon Nanotubes *via* Grafting-from Method. *Chem. Lett.* **2004**, *33*, 490–491.
38. García, A.; Herrero, M. A.; Frein, S.; Deschenaux, R.; Muñoz, R.; Bustero, I.; Toma, F.; Prato, M. Synthesis of Dendrimer−Carbon Nanotube Conjugates. *Phys. Status Solidi A* **2008**, *205*, 1402–1407.
39. Sun, Y. P.; Huang, W.; Lin, Y.; Fu, K.; Kitaygorodskiy, A.; Riddle, L. A.; Joy Yu, Y.; Carroll, D. L. Soluble Dendron-Functionalized Carbon Nanotubes: Preparation, Characterization, and Properties. *Chem. Mater.* **2001**, *13*, 2864–2869.
40. Jiang, G. H.; Wang, L.; Chen, C.; Dong, X.; Chen, T.; Yu, H. Study on Attachment of Highly Branched Molecules onto Multiwalled Carbon Nanotubes. *Mater. Lett.* **2005**, *59*, 2085–2089.
41. Herrero, M. A.; Toma, F. M.; Al-Jamal, K. T.; Kostarelos, K.; Bianco, A.; Da Ros, T.; Bano, F.; Casalis, L.; Scoles, G.; Prato, M. Synthesis and Characterization of a Carbon Nanotube-Dendron Series for Efficient siRNA Delivery. *J. Am. Chem. Soc.* **2009**, *131*, 9843–9848.
42. Hwang, S. H.; Moorefield, C. N.; Wang, P.; Jeong, K.-U.; Cheng, S. Z. D.; Kotta, K. K.; Newkome, G. R. Dendron-Tethered and Templated CdS Quantum Dots on Single-Walled Carbon Nanotubes. *J. Am. Chem. Soc.* **2006**, *128*, 7505–7509.
43. Lu, X.; Imae, T. Size-Controlled *In Situ* Synthesis of Metal Nanoparticles on Dendrimer-Modified Carbon Nanotubes. *J. Phys. Chem. C* **2007**, *111*, 2416–2420.
44. Lu, X.; Imae, T. Dendrimer-Mediated Synthesis of Water-Dispersible Carbon-Nanotube-Supported Oxide Nanoparticles. *J. Phys. Chem. C* **2007**, *111*, 8459–8462.
45. Vijayaraghavan, G.; Stevenson, K. J. Synergistic Assembly of Dendrimer-Templated Platinum Catalysts on Nitrogen-Doped Carbon Nanotube Electrodes for Oxygen Reduction. *Langmuir* **2007**, *23*, 5279–5282.

46. Georgakilas, V.; Gournis, D.; Tzitzios, V.; Pasquato, L.; Guldi, D. M.; Prato, M. Decorating Carbon Nanotubes with Metal or Semiconductor Nanoparticles. *J. Mater. Chem.* **2007**, *17*, 2679–2694.
47. Yuan, W.; Jiang, G.; Che, J.; Qi, X.; Xu, R.; Chang, M. W.; Chen, Y.; Lim, S. Y.; Dai, J.; Chan-Park, M. B. Deposition of Silver Nanoparticles on Multiwalled Carbon Nanotubes Grafted with Hyperbranched Poly(amidoamine) and Their Antimicrobial Effects. *J. Phys. Chem. C* **2008**, *112*, 18754–18759.
48. Zenga, Y.; Tang, C.; Wang, H.; Jiang, J.; Tian, M.; Shen, G.; Yu, R. A Novel Density-Tunable Nanocomposites of CdTe Quantum Dots Linked to Dendrimer-Tethered Multi-Wall Carbon Nanotubes. *Spectrochim. Acta, Part A* **2008**, *70*, 966–972.
49. Garcia, M. E.; Baker, L. A.; Crooks, R. M. Preparation and Characterization of Dendrimer-Gold Colloid Nanocomposites. *Anal. Chem.* **1999**, *71*, 256–258.
50. Podesta, J. E.; Al-Jamal, K. T.; Herrero, M. A.; Tian, B.; Ali-Boucetta, H.; Hegde, V.; Bianco, A.; Prato, M.; Kostarelos, K. Antitumor Activity and Prolonged Survival by Carbon-Nanotube-Mediated Therapeutic siRNA Silencing in a Human Lung Xenograft Model. *Small* **2009**, *5*, 1176–1185.
51. Mintzer, M. A.; Simanek, E. E. Nonviral Vectors for Gene Delivery. *Chem. Rev.* **2009**, *109*, 259–302.
52. Boas, U.; Christensen, J. B.; Heegaard, P. M. H. *Dendrimers in Medicine and Biotechnology. New Molecular Tools*; RSC Publishing: London, 2006.
53. Svenson, S.; Tomalia, D. A. Dendrimers in Biomedical Applications—Reflections on the Field. *Adv. Drug Delivery Rev.* **2005**, *57*, 2106–2129.
54. Caminade, A. M.; Turrin, C. O.; Majoral, J. P. Dendrimers and DNA: Combinations of Two Special Topologies for Nanomaterials and Biology. *Chem.—Eur. J.* **2008**, *14*, 7422–7432.
55. Dufes, C.; Uchegbu, I. F.; Schatzlein, A. G. Dendrimers in Gene Delivery. *Adv. Drug Delivery Rev.* **2005**, *57*, 2177–2202.
56. Kim, Y. G.; Oh, S. K.; Crooks, R. M. Preparation and Characterization of 1−2 nm Dendrimer-Encapsulated Gold Nanoparticles Having Very Narrow Size Distributions. *Chem. Mater.* **2004**, *16*, 167–172.
57. Wu, W.; Wieckowski, S.; Pastorin, G.; Benincasa, M.; Klumpp, C.; Briand, J. P.; Gennaro, R.; Prato, M.; Bianco, A. Targeted Delivery of Amphotericin B to Cells by Using Functionalized Carbon Nanotubes. *Angew. Chem., Int. Ed.* **2005**, *44*, 6358–6362.
58. Hu, H.; Bhowmik, P.; Zhao, B.; Hamon, M. A.; Itkis, M. E.; Haddon, R. C. Determination of the Acidic Sites of Purified Single-Walled Carbon Nanotubes by Acid−Base Titration. *Chem. Phys. Lett.* **2001**, *345*, 25–28.
59. Mawhinney, D. B.; Naumenko, V.; Kuznetsova, A.; Yates, J. T.; Liu, J.; Smalley, R. E. Surface Defect Site Density on Single Walled Carbon Nanotubes by Titration. *Chem. Phys. Lett.* **2000**, *324*, 213–216.
60. Hirsch, A. Functionalization of Single-Walled Carbon Nanotubes. *Angew. Chem., Int. Ed.* **2002**, *41*, 1853–1859.
61. Liu, J.; Casavant, M. J.; Cox, M.; Walters, D. A.; Boul, P.; Lu, W.; Rimberg, A. J.; Smith, K. A.; Colbert, D. T.; Smalley, R. E. Controlled Deposition of Individual Single-Walled Carbon Nanotubes on Chemically Functionalized Templates. *Chem. Phys. Lett.* **1999**, *303*, 125–129.
62. Gallardo, I.; Pinson, J.; Vila, N. Spontaneous Attachment of Amines to Carbon and Metallic Surfaces. *J. Phys. Chem. B* **2006**, *110*, 19521–19529.
63. Sun, L.; Crooks, R. M. Dendrimer-Mediated Immobilization of Catalytic Nanoparticles on Flat, Solid Supports. *Langmuir* **2002**, *18*, 8231–8236.
64. Garcia-Gutierrez, D.; Gutierrez-Wing, C.; Miki-Yoshida, M.; Jose-Yacamán, M. HAADF Study of Au−Pt Core−Shell Bimetallic Nanoparticles. *Appl. Phys. A: Mater. Sci. Process.* **2004**, *79*, 481–487.
65. Shukla, R.; Hill, E.; Shi, X.; Kim, J.; Muniz, M. C.; Sun, K.; Baker, J. R., Jr. Tumor Microvasculature Targeting with Dendrimer-Entrapped Gold Nanoparticles. *Soft Matter* **2008**, *4*, 2160–2163.
66. Ozturk, O.; Black, T. J.; Perrine, K.; Pizzolato, K.; Williams, C. T.; Parsons, F. W.; Ratliff, J. S.; Gao, J.; Murphy, C. J.; Xie, H.; Ploehn, H. J.; Chen, D. A. Thermal Decomposition of Generation-4 Polyamidoamine Dendrimer Films: Decomposition Catalyzed by Dendrimer-Encapsulated Pt Particles. *Langmuir* **2005**, *21*, 3998–4006.
67. Lang, H.; May, R. A.; Iversen, B. L.; Chandler, B. D. Dendrimer-Encapsulated Nanoparticle Precursors to Supported Platinum Catalysts. *J. Am. Chem. Soc.* **2003**, *125*, 14832–14836.
68. Deutsch, D. S.; Lafaye, G.; Liu, D.; Chandler, B.; Williams, C. T.; Amiridis, M. D. Decomposition and Activation of Pt-Dendrimer Nanocomposites on a Silica Support. *Catal. Lett.* **2004**, *97*, 139–143.
69. Pang, L. S. K.; Saxby, J. D.; Chatfield, S. P. Thermogravimetric Analysis of Carbon Nanotubes and Nanoparticles. *J. Phys. Chem.* **1993**, *97*, 6941–6942.
70. Kaiser, E.; Colescot, R. L.; Bossinge, C. D.; Cook, P. I. Color Test for Detection of Free Terminal Amino Groups in Solid-Phase Synthesis of Peptides. *Anal. Biochem.* **1970**, *34*, 595–598.
71. Sarin, V. K.; Kent, S. B. H.; Tam, J. P.; Merrifield, R. B. Quantitative Monitoring of Solid-Phase Peptide Synthesis by the Ninhydrin Reaction. *Anal. Biochem.* **1981**, *117*, 147–157.
72. Deutsch, D. S.; Siani, A.; Fanson, P. T.; Hirata, H.; Matsumoto, S.; Williams, C. T.; Amiridis, M. D. FT-IR Investigation of the Thermal Decomposition of Poly(amidoamine) Dendrimers and Dendrimer-Metal Nanocomposites Supported on Al_2O_3 and ZrO. *J. Phys. Chem. C* **2007**, *111*, 4246–4255.
73. He, M.; McLuckey, S. A. Tandem Mass Spectrometry of Half-Generation PAMAM Dendrimer Anions. *Rapid Commun. Mass Spectrom.* **2004**, *18*, 960–972.
74. Peterson, J.; Allikmaa, V.; Pehk, T.; Lopp, M. Fragmentation of PAMAM Dendrimers in Methanol. *Proc. Estonian Acad. Sci. Chem.* **2001**, *50*, 167–172.
75. Peterson, J.; Allikmaa, V.; Subbi, J.; Pehk, T.; Lopp, M. Structural Deviations in Poly(amidoamine) Dendrimers: A MALDI-TOF MS Analysis. *Eur. Polym. J.* **2003**, *39*, 33–42.
76. Vincent, T. J.-C.; Dole, R.; Lange, C. M. Gas-Phase Fragmentation of Half- and First-Generation Polyamidoamine Dendrimers by Electrospray Mass Spectrometry Using a Quadrupole Ion Trap. *Rapid Commun. Mass Spectrom.* **2008**, *22*, 363–372.
77. Gomez, M. V.; Guerra, J.; Velders, A. H.; Crooks, R. M. Manuscript in preparation.
78. Antalek, B. Using Pulsed Gradient Spin Echo NMR for Chemical Mixture Analysis: How to Obtain Optimum Results. *Concepts Magn. Reson., Part A* **2002**, *14*, 225–258.